Title: Loop Quantum Gravity and High Energy Cosmic Rays

Date: Oct 31, 2004 09:35 AM

URL: http://pirsa.org/04100045

Abstract:

3. Cosmic Rays Spectrum

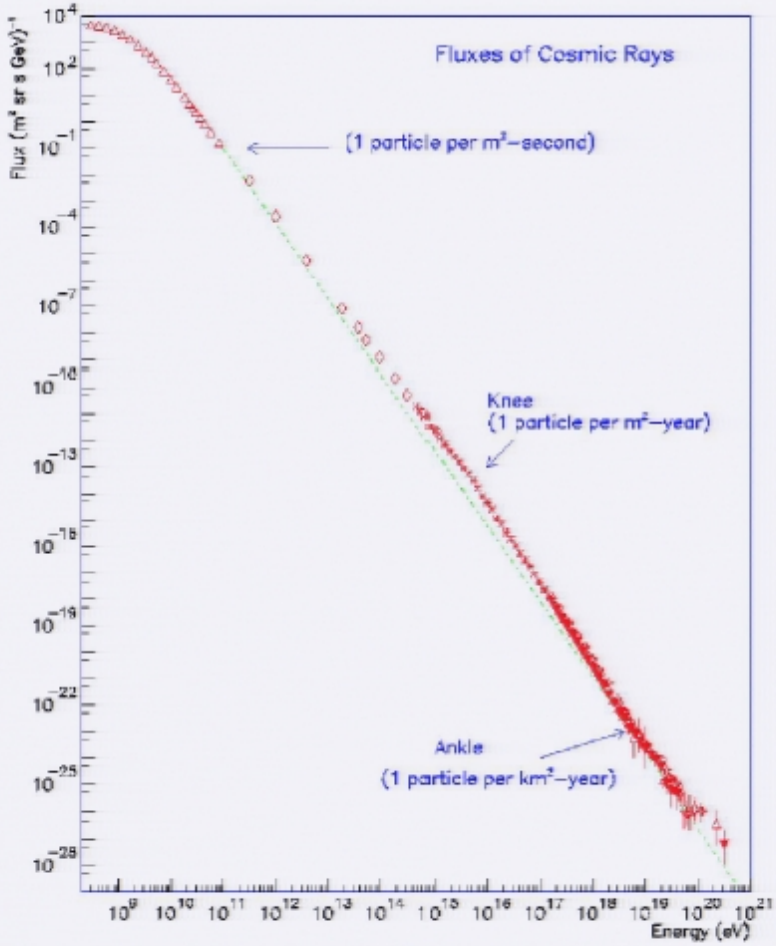

Assumption: Sources emit according to: $F(E) \sim E^{-\gamma_g}$ where γ_g is the generation index.$\gamma_g = 2.7$, $E < 4 \times 10^{15}$eV; $\gamma_g = 3.2$, $4 \times 10^{15} < E < 4 \times 10^{18}$eV; $\gamma_g = 2.7$, $E < 4 \times 10^{18}$eV.

4. Cosmic Background Radiation

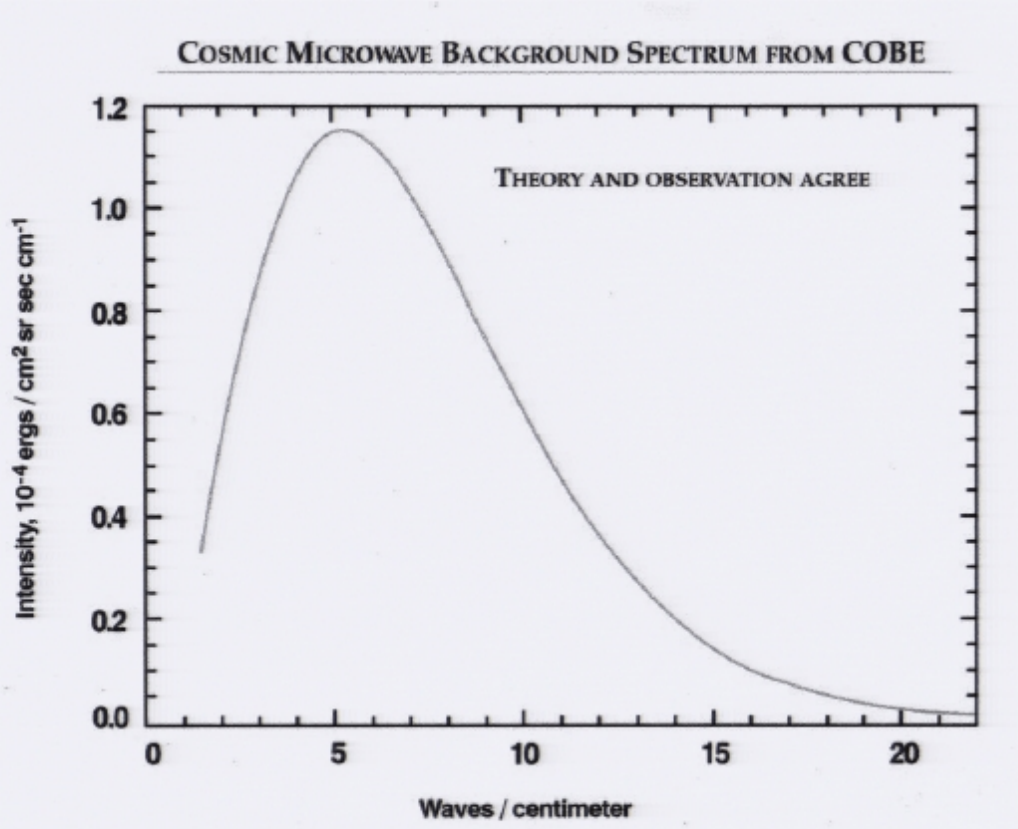

5. High Energy Cosmic Rays

- In this talk we are concerned with the observation of ultra high energy cosmic rays (UHECR), i.e. those cosmic rays with energies greater than $\sim 4 \times 10^{18}$ eV.
- Although not completely clear, it has been suggested that these high energy particles are possibly heavy nuclei (we will assume here that they are protons).
- By virtue of the isotropic distribution with which they arrive to us, they originate in extragalactic sources.

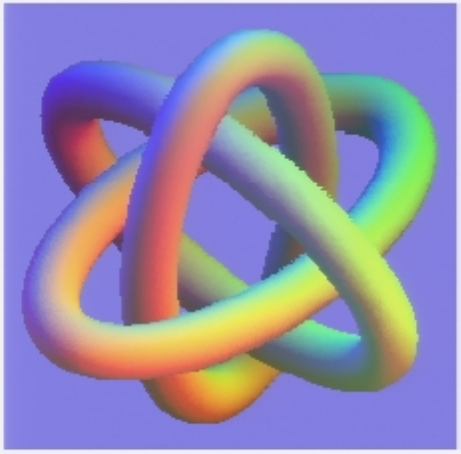

6. The Greisen-Zatsepin-Kuz'min (GZK) cutoff

- Their propagation in open space is affected by the cosmic microwave background radiation (CMBR), producing a friction on UHECR making them release energy in the form of secondary particles and affecting their possibility to reach great distances.
- Cosmic rays with energies above 1×10^{20} eV should not travel more than ~ 100 Mpc.

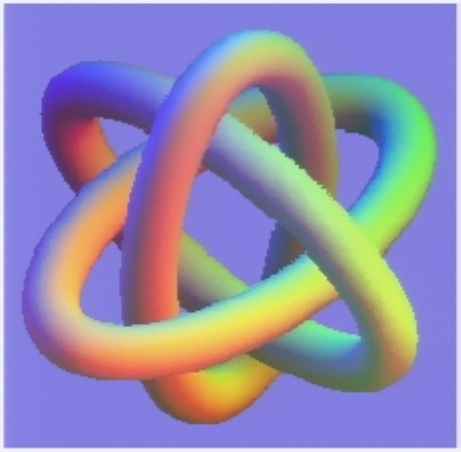

7. HIRES Data

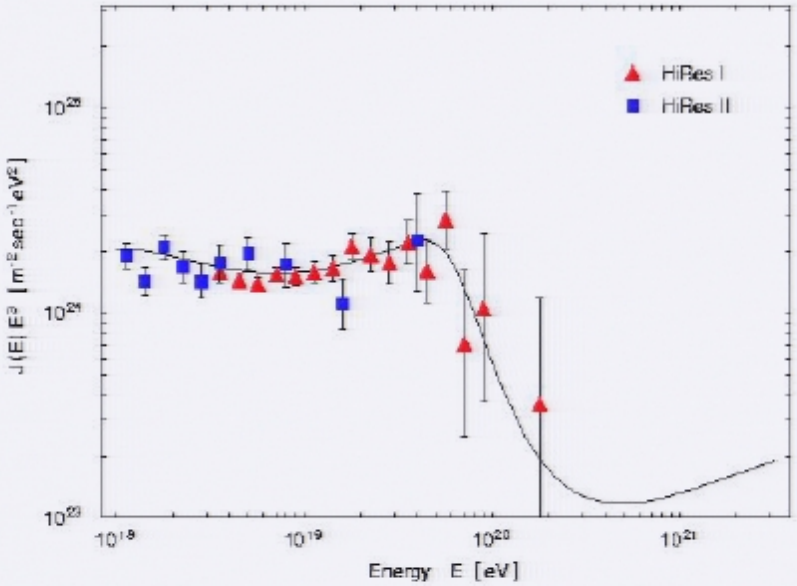

UHECR spectrum and HiRes observations. The figure shows the UHECR spectrum $J(E)$ multiplied by E^3, for uniform distributed sources, without evolution ($m = 0$), generation index $\gamma_g = 2.7$, and with a maximum generation energy $E_{\max} = \infty$. Also shown are the HiRes observed events.

6. The Greisen-Zatsepin-Kuz'min (GZK) cutoff

- Their propagation in open space is affected by the cosmic microwave background radiation (CMB), producing a friction on UHECR making them release energy in the form of secondary particles and affecting their possibility to reach great distances.
- Cosmic rays with energies above 1×10^{20} eV should not travel more than ~ 100 Mpc.

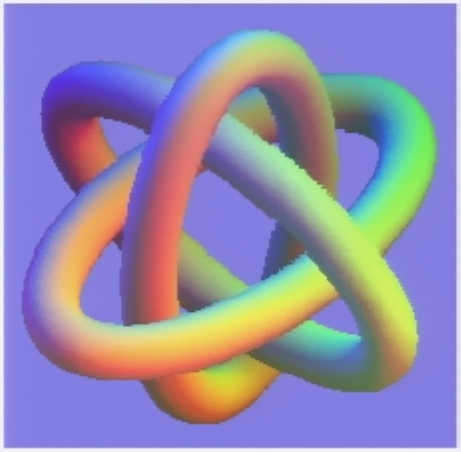

7. HIRES Data

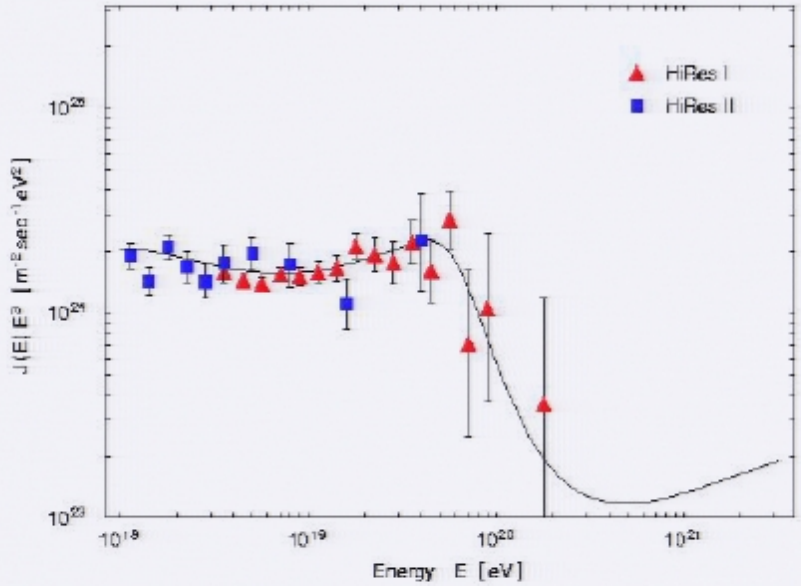

UHECR spectrum and HiRes observations. The figure shows the UHECR spectrum $J(E)$ multiplied by E^3, for uniform distributed sources, without evolution ($m = 0$), generation index $\gamma_g = 2.7$, and with a maximum generation energy $E_{\max} = \infty$. Also shown are the HiRes observed events.

8. AGASA Data

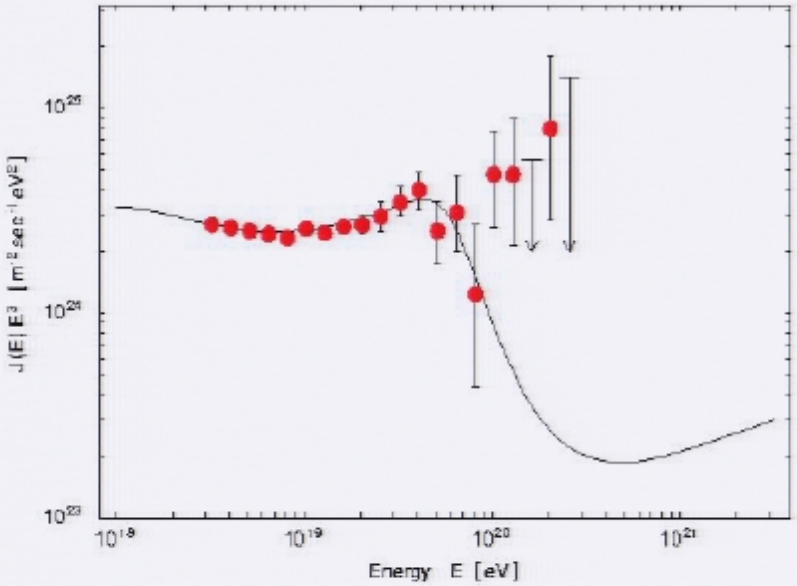

The figure shows the UHECR spectrum $J(E)$ multiplied by E^3, for uniform distributed sources, without evolution, and with a maximum generation energy $E_{\max} = \infty$. Also shown are the AGASA observed events. The best fit for the low energy sector ($E < 4 \times 10^{19}$ eV) corresponds to $\gamma_g = 2.7$.

9. Discrete Geometry

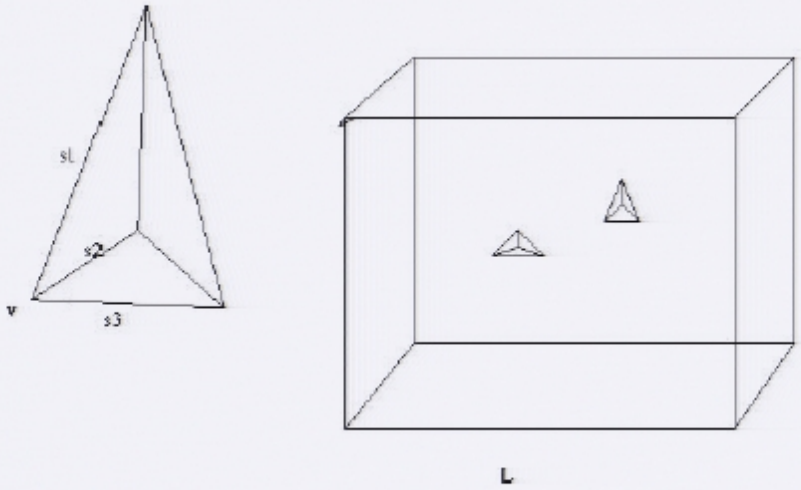

The figure shows a discrete random geometry. $s_i \sim l_P \sim 10^{-33}$cm. L=$\mathcal{L}$ is the characteristic length scale of the semiclassical LQG state. $l_P << \mathcal{L} << \frac{h}{p}$.
For $d << \mathcal{L}$, the geometry is discrete.
For $d >> \mathcal{L}$, we recover the continuum geometry.$\mathcal{L}^3 \sim d^3x$

10. Dispersion Relations

In what follows, it will be sufficient to consider for fermions

$$E_{\pm}^2 = A^2 p^2 + \kappa_3 \, \ell_p^2 \, p^4 \pm \kappa_5 \frac{\ell_p}{\mathcal{L}^2} \mathrm{p} + m^2 + \frac{1}{4} \left(\kappa_5 \frac{\ell_p}{\mathcal{L}^2} \right)^2 , \tag{1}$$

where now $A = 1 + \kappa_1 \, \ell_p / \mathcal{L}$ and κ_1, κ_3 and κ_5 are of order one. For simplicity, let us write (with $\eta = \kappa_3 \ell_p^2$ and $\lambda = \kappa_5 \ell_p / 2\mathcal{L}^2$)

$$E_{\pm}^2 = A^2 p^2 + \eta p^4 \pm 2\lambda p + m^2, \tag{2}$$

As before, we note the presence of the $\pm$ signs which denote the helicity dependance of the fermion. To the order of interest, for photons we have the following dispersion relations:

$$E_{\pm}^2 = p^2 \left[A_\gamma^2 \pm 2\theta_\gamma (\ell_p p) \right] . \tag{3}$$

Notably, (3) is essentially the same result that Gambini and Pullin have obtained for photon's dispersion relation, with the difference that they have $A_\gamma = 1$ and therefore the semiclassical scale $\mathcal{L}$ is absent.

11. Bounds on the LID parameters

- 1) We have seen that the conventionally obtained theoretical spectrum provides a very good description of the phenomena up to an energy $\sim 4 \times 10^{19}$ eV. The main reaction taking place in this well described region is the pair creation $\gamma + p \rightarrow p + e^+ + e^-$.

  So, we will require that the threshold condition for pair creation not be substantially altered by the new corrective terms.

- 2) Since for energies greater than $\sim 8 \times 10^{19}$ eV the conventional theoretical spectrum does not fit the experimental data well, we shall require that LQG corrections be able to offer a violation of the GZK-cutoff.

  The dominant reaction in the violated $E > 8 \times 10^{19}$ region is the photo-pion production and, therefore, we shall require further that the new corrective terms present in the kinematical calculations be able to shift the threshold significantly to preclude the reaction.

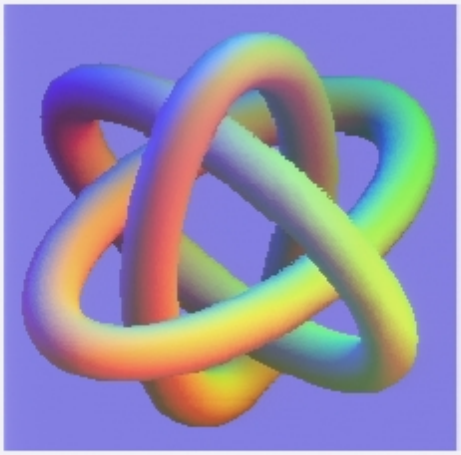

8. AGASA Data

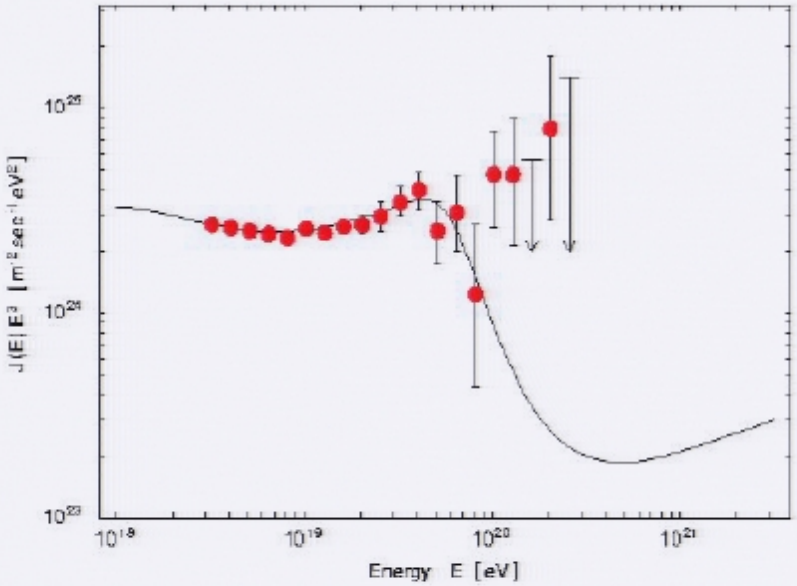

The figure shows the UHECR spectrum $J(E)$ multiplied by E^3, for uniform distributed sources, without evolution, and with a maximum generation energy $E_{\max} = \infty$. Also shown are the AGASA observed events. The best fit for the low energy sector ($E < 4 \times 10^{19}$ eV) corresponds to $\gamma_g = 2.7$.

11. Bounds on the LID parameters

- 1) We have seen that the conventionally obtained theoretical spectrum provides a very good description of the phenomena up to an energy $\sim 4 \times 10^{19}$ eV. The main reaction taking place in this well described region is the pair creation $\gamma + p \rightarrow p + e^+ + e^-$.

  So, we will require that the threshold condition for pair creation not be substantially altered by the new corrective terms.

- 2) Since for energies greater than $\sim 8 \times 10^{19}$ eV the conventional theoretical spectrum does not fit the experimental data well, we shall require that LQG corrections be able to offer a violation of the GZK-cutoff.

  The dominant reaction in the violated $E > 8 \times 10^{19}$ region is the photo-pion production and, therefore, we shall require further that the new corrective terms present in the kinematical calculations be able to shift the threshold significantly to preclude the reaction.

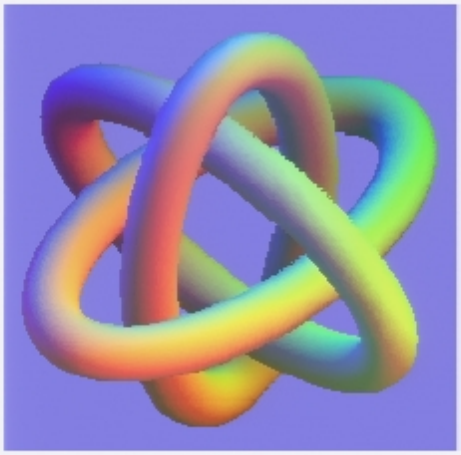

12. The Cubic Correction

A commonly studied correction which has appeared in several recent works, and which deserves our attention, is the case of a cubic correction of the form

$$E^2 = p^2 + m^2 + \xi\, p^3, \tag{4}$$

(where ξ is an arbitrary scale). It is interesting to note that strong bounds can be placed over deformation $f(p) = \xi\, p^3$. We will assume in this section, that ξ is an universal parameter (an assumption followed by most of the works in this field).

$$\begin{aligned} \xi \;<\; & \frac{(m_p + m_e)(m_p + 2m_e)^2}{m_p\, E_{\rm ref}^3} \\ & = 3.26 \times 10^{-41}\ {\rm eV}^{-1} \\ & (= 3.98 \times 10^{-13}\, l_p), \end{aligned} \tag{5}$$

where we have used $E_{\rm ref} = 3 \times 10^{19}$ eV. This last result shows the strong suppression over ξ. As a consequence, the particular case $\xi = l_p = 8 \times 10^{-28}\ {\rm eV}^{-1}$ should be discarded.

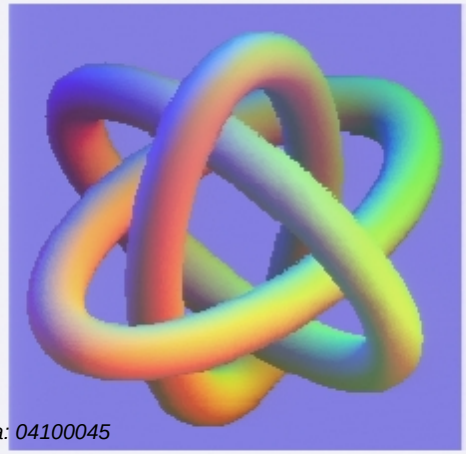

13. Cosmic Rays Spectrum

Two simple and commonly used assumptions for the development of the cosmic ray spectrum are:

- -1) The sources are uniformly distributed in the Universe,
- -2) The generation flux $F(E_g)$ of emitted cosmic rays from the sources is correctly described by a power law behavior of the form $F(E_g) \propto E_g^{-\gamma_g}$, where E_g is the energy of the emitted particle and γ_g is the generation index.

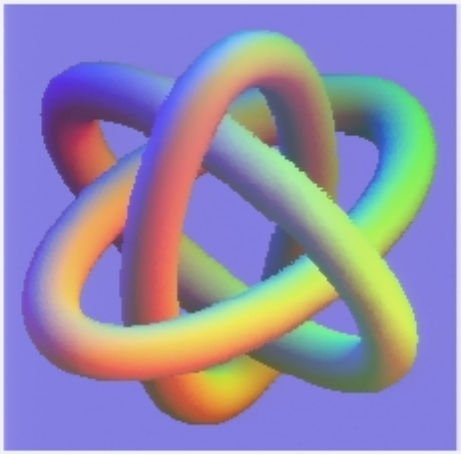

14. Modified Spectrum of High Energy Cosmic Rays

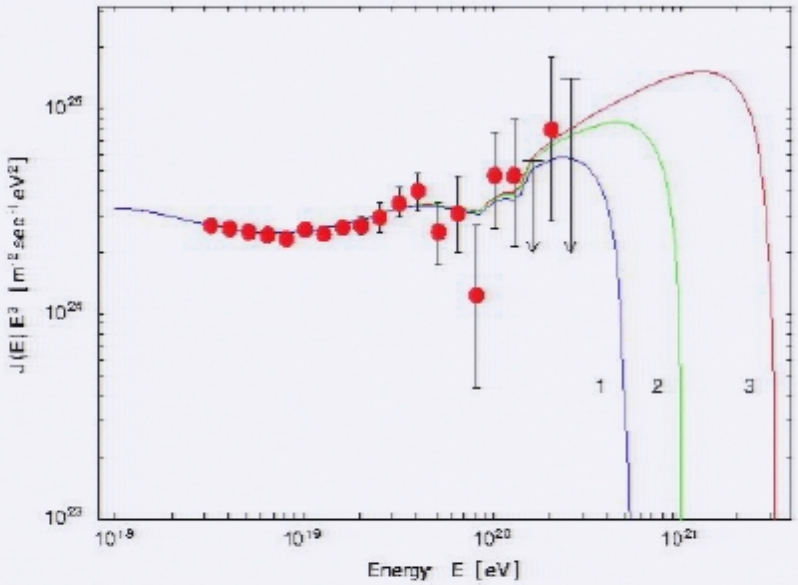

Modified UHECR spectrum and AGASA observations. The figure shows the modified spectrum $J(E)$ multiplied by E^3, for uniform distributed sources and without evolution, for the case $\alpha_m = 1.5 \times 10^{-22}$ ($\mathcal{L} \simeq 6.7 \times 10^{-18}$ eV^{-1}). Three different maximum generation energies $E_{\max}$ are shown. These are, curve 1: 5×10^{20} eV; curve 2: 1×10^{21} eV; and curve 3: 3×10^{21} eV.

10. Dispersion Relations

In what follows, it will be sufficient to consider for fermions

$$E_{\pm}^2 = A^2 p^2 + \kappa_3 \, \ell_p^2 \, p^4 \pm \kappa_5 \frac{\ell_p}{\mathcal{L}^2} \mathrm{p} + m^2 + \frac{1}{4} \left(\kappa_5 \frac{\ell_p}{\mathcal{L}^2} \right)^2 , \tag{1}$$

where now $A = 1 + \kappa_1 \, \ell_p / \mathcal{L}$ and κ_1, κ_3 and κ_5 are of order one. For simplicity, let us write (with $\eta = \kappa_3 \ell_p^2$ and $\lambda = \kappa_5 \ell_p / 2\mathcal{L}^2$)

$$E_{\pm}^2 = A^2 p^2 + \eta p^4 \pm 2\lambda p + m^2, \tag{2}$$

As before, we note the presence of the $\pm$ signs which denote the helicity dependance of the fermion. To the order of interest, for photons we have the following dispersion relations:

$$E_{\pm}^2 = p^2 \left[A_\gamma^2 \pm 2\theta_\gamma (\ell_p p) \right] . \tag{3}$$

Notably, (3) is essentially the same result that Gambini and Pullin have obtained for photon's dispersion relation, with the difference that they have $A_\gamma = 1$ and therefore the semiclassical scale $\mathcal{L}$ is absent.

14. Modified Spectrum of High Energy Cosmic Rays

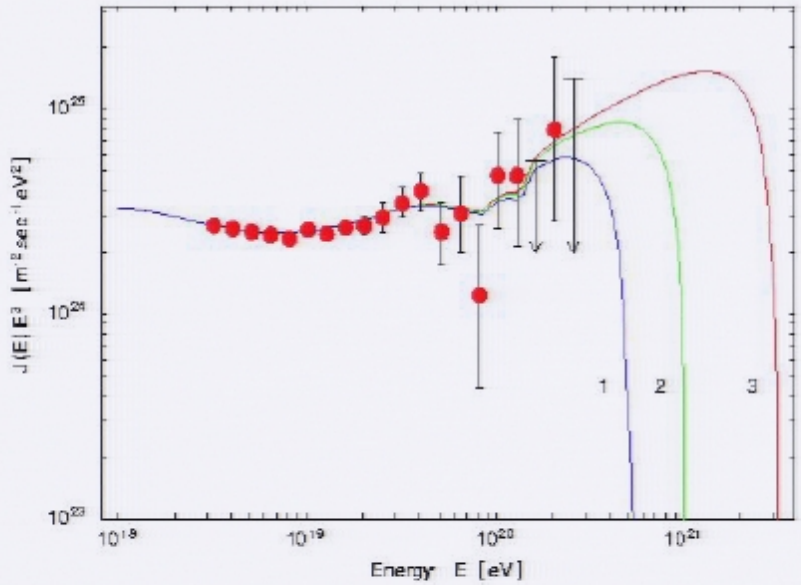

Modified UHECR spectrum and AGASA observations. The figure shows the modified spectrum $J(E)$ multiplied by E^3, for uniform distributed sources and without evolution, for the case $\alpha_m = 1.5 \times 10^{-22}$ ($\mathcal{L} \simeq 6.7 \times 10^{-18}$ eV^{-1}). Three different maximum generation energies $E_{\max}$ are shown. These are, curve 1: 5×10^{20} eV; curve 2: 1×10^{21} eV; and curve 3: 3×10^{21} eV.

13. Cosmic Rays Spectrum

Two simple and commonly used assumptions for the development of the cosmic ray spectrum are:

- -1) The sources are uniformly distributed in the Universe,
- -2) The generation flux $F(E_g)$ of emitted cosmic rays from the sources is correctly described by a power law behavior of the form $F(E_g) \propto E_g^{-\gamma_g}$, where E_g is the energy of the emitted particle and γ_g is the generation index.

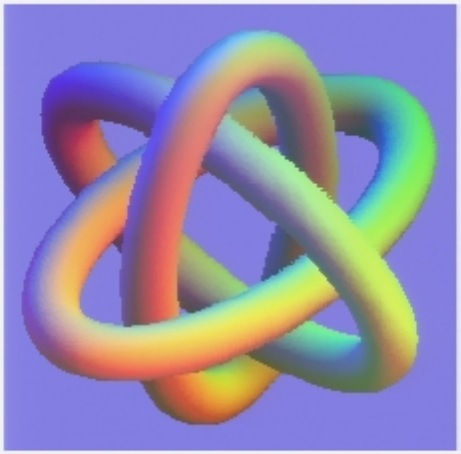

15. CONCLUSIONS

- We have studied the propagation of massive particles and photons in the context of Loop Quantum Gravity.
- **The discrete structure of space to the scale of $l_P \sim 10^{-33}$ cm produces corrections to the macroscopic propagation of the particles.**
- We have seen how the kinematical analysis of the different reaction taking place in the propagation of ultra high energy protons can set strong bounds on the parameters to the theory. In comparison with our previous work, we have eliminated some previously open possibilities by the particular study of the pair creation $p+\gamma \rightarrow p+e^+ +e^-$, in the energy region where this reaction dominates the proton's interactions with the CMBR. In this way, the only possibility still open (for the corrective terms considered in the expansion for the dispersion relations) and favored by the LQG scales, is the correction α. If this is the case, a favored region for the scale length $\mathcal{L}$ estimated through the threshold analysis would be

$$2.6 \times 10^{-18}\ \text{eV}^{-1} <= \mathcal{L} <= 1.6 \times 10^{-17}\ \text{eV}^{-1}.$$

16. Future Perspective

- Future experimental developments like the Auger array, the Extreme Universe Space Observatory (EUSO) and Orbiting Wide-Angle Light Collectors (OWL) satellite detectors, will increase the precision and phenomenological description of UHECR.
- On the more theoretical side, progress in the direction of a full effective theory, with a systematic method to compute any correction with a known value for each coefficient, is one of the next steps in the "loop" quantization programme.
- This will set stronger bounds on the parameter of the theory and decide if the quantum gravity corrections to the propagation of particles is our first direct evidence of a Quantum Theory of Gravity.

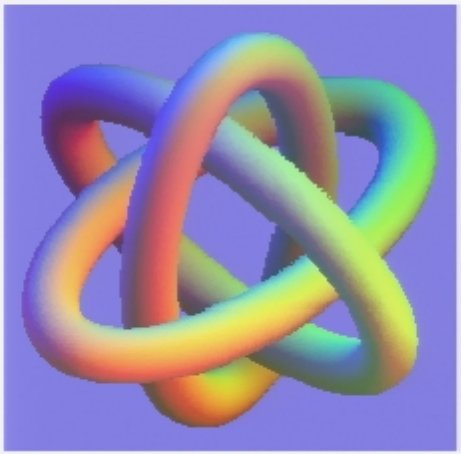

16. Future Perspective

- Future experimental developments like the Auger array, the Extreme Universe Space Observatory (EUSO) and Orbiting Wide-Angle Light Collectors (OWL) satellite detectors, will increase the precision and phenomenological description of UHECR.
- On the more theoretical side, progress in the direction of a full effective theory, with a systematic method to compute any correction with a known value for each coefficient, is one of the next steps in the "loop" quantization programme.
- This will set stronger bounds on the parameter of the theory and decide if the quantum gravity corrections to the propagation of particles is our first direct evidence of a Quantum Theory of Gravity.

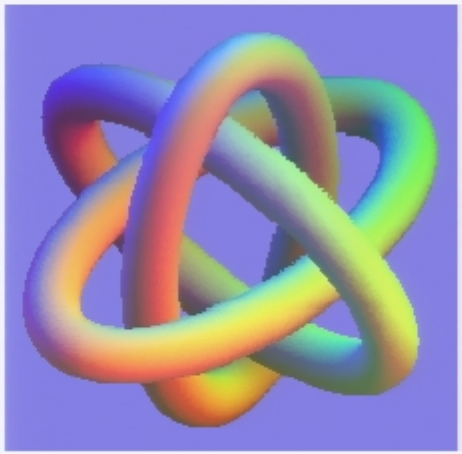

16. Future Perspective

- Future experimental developments like the Auger array, the Extreme Universe Space Observatory (EUSO) and Orbiting Wide-Angle Light Collectors (OWL) satellite detectors, will increase the precision and phenomenological description of UHECR.
- On the more theoretical side, progress in the direction of a full effective theory, with a systematic method to compute any correction with a known value for each coefficient, is one of the next steps in the "loop" quantization programme.
- This will set stronger bounds on the parameter of the theory and decide if the quantum gravity corrections to the propagation of particles is our first direct evidence of a Quantum Theory of Gravity.